Understanding the State of the Intracluster Medium in Galaxy Clusters

A White Paper for the

Galaxies Across Cosmic Time Science Frontier Panel

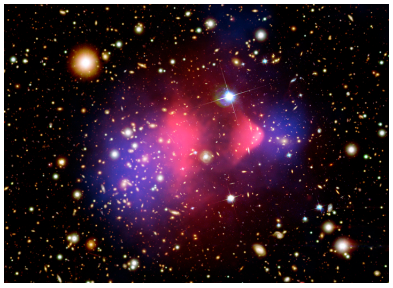

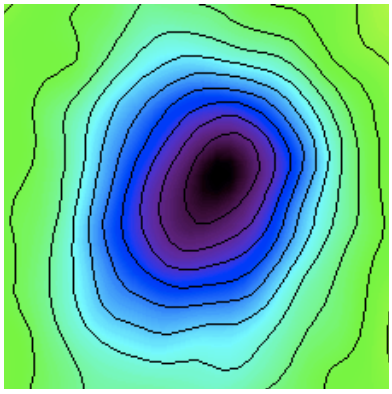

Optical, weak lensing (blue), and Chandra X-ray (red) image and South Pole Telescope thermal Sunyaev-Zeldovich effect map of the Bullet Cluster ([1], SPT Collaboration).

S. R. Golwala* (Caltech), J. E. Aguirre (U. Penn.), K. Basu (U. Bonn, MPIfR Bonn),
B. A. Benson (U. Chicago), F. Bertoldi (U. Bonn), J. O. Burns (U. Colorado),
S. E. Church (Stanford), M. J. Devlin (U. Penn.), M. Dobbs (McGill),
J. W. Fowler (Princeton), E. J. Hallman (U. Colorado), W. L. Holzapfel (Berkeley),
A. V. Kravtsov (U. Chicago), A. T. Lee (Berkeley), D. P. Marrone (U. Chicago),
B. S. Mason (NRAO), A. D. Miller (Columbia), S. T. Myers (NRAO),
D. Nagai (Yale), M. Nord (U. Bonn), L. Page (Princeton),
C. Pfrommer (CITA), E. Pierpaoli (USC), J. E. Ruhl (CWRU),
G. W. Wilson (U. Mass, Amherst)

*contact author, golwala@caltech.edu, 626-395-8003

Introduction

Galaxy clusters are intrinsically interesting astrophysical objects. Their formation involves an enormous amount of energy conversion and thus produces systems with large concentrations of galaxies and large amounts of highly heated plasma, rendering clusters visible in many different observing bands over a wide range of redshifts. Given that clusters collapse from a large region (∼10 Mpc), their contents are expected to reflect the overall properties of the universe and thus clusters are expected to have relatively predictable behavior. But astronomers also want to be able to quantitatively predict the ensemble, large-scale deviations from self-similar behavior of galaxy clusters based on fundamental physics and our understanding of galaxy evolution and galaxy interactions with the intracluster medium (ICM). Conversely, clusters are important tools for understanding how the ICM, and the environment in general, affects the evolution of galaxies and the supermassive black holes they harbor. An understanding of clusters necessarily involves measurements and predictions of the structure of the underlying dark matter, the gaseous ICM, and the galaxies themselves (see companion white paper by Myers *et al.* for a survey of cluster studies [2]). Focusing on the ICM, advances in the next decade in observational capabilities and theoretical models can address one of the key questions of cluster astrophysics: **What is the thermodynamic state of the intracluster medium?** Specifically, what are the detailed position dependences of the ICM density and temperature, how do they deviate from self-similar behavior, and to what extent are there non-thermal components? Precise observations of the ICM via X-ray emission and the thermal Sunyaev-Zeldovich (tSZ) effect can answer this question.

The Current Understanding of Clusters

According to our current understanding, galaxy clusters are composed of: a dark matter halo that dominates the gravitational potential; a hot, gaseous, baryonic ICM close to hydrostatic equilibrium in the potential well (∼10% by mass); and a population of galaxies (∼1% by mass). The most massive clusters have gas temperatures of $kT \approx 10$–15 keV, masses of $\sim 5 \times 10^{15}$ $M_\odot$, and virial radii of $R_{vir} = 3$–4 Mpc. The border between clusters and groups lies at approximately 10^{14} $M_\odot$ ($kT \sim 1$ keV and $R_{vir} \sim 1.5$ Mpc). Clusters are largely regular objects, exhibiting tight correlations between global properties of their various components (Figure 1) that are expected from self-similar (*i.e.*, gravity only) collapse and are confirmed in simulations [3, 4, 5]. However, Figure 1 also shows important deviations from this simple picture: including non-gravitational processes like radiative cooling and star formation in member galaxies results in a better match to the data than do self-similar models. Nevertheless, discrepancies remain and a variety of nongravitational effects are not yet included, such as thermal conduction, turbulence, stellar winds and AGN jets, tidal and ram pressure stripping of gas, magnetic field support, and cosmic ray pressure.

Studying the Intracluster Medium

A comprehensive understanding of the ICM requires: 1) direct measurement of the thermodynamic state of the ICM; 2) observations to reveal and quantify non-self-similar phenomena; and 3) simulations that include both gravitational and relevant non-self-similar processes.

The first area consists of observations of the ICM itself that characterize deviations from self-similar behavior. X-ray imaging provides a calorimetric measurement of thermal emission

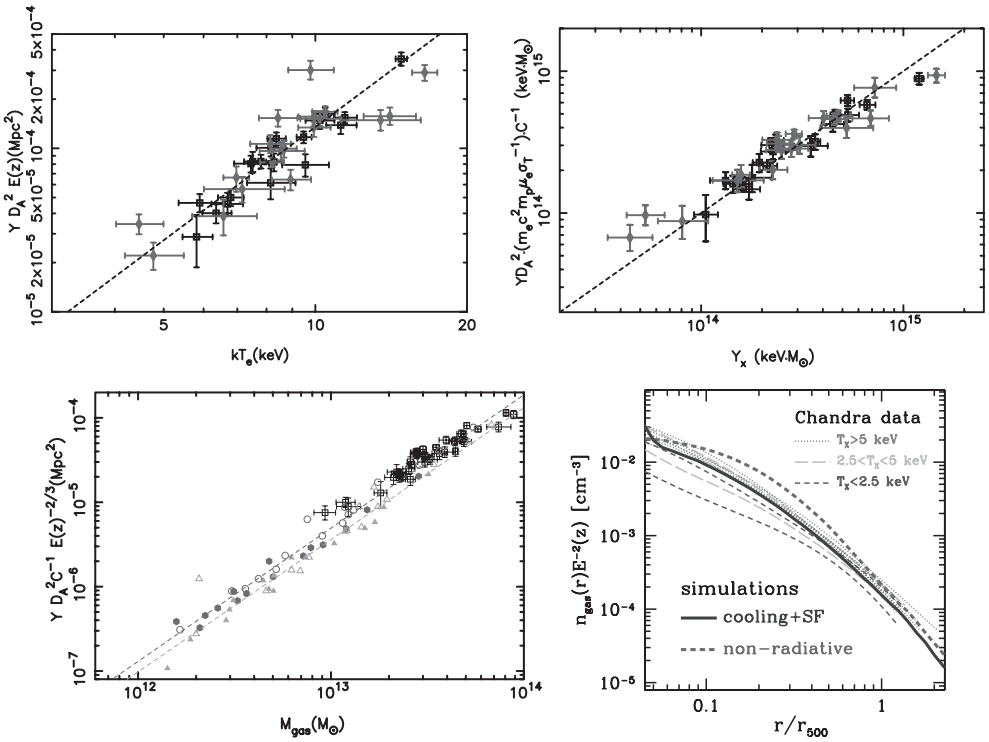

Figure 1: Top: Example scaling relations [6]. Top left: integrated SZ Comptonization $Y\,D_A^2$ (proportional to integrated tSZ flux) vs. X-ray temperature. Top right: $Y\,D_A^2$, in different units, vs. $Y_X = M_{gas}\,k\,T$. Bottom left: Comparison of integrated SZ Comptonization vs. gas mass scaling relation to simulations [6]. Points with error bars are data. Triangles: self-similar simulations; circles/hexagons: simulations including radiative cooling and star formation feedback. Open and filled symbols: $z = 0$ and $z = 0.6$ simulated clusters, respectively. Dashed lines: power law fits to the self-similar and non-self-similar models. The non-self-similar model is favored by χ^2 tests. Bottom right: X-ray-derived gas density vs. radius for simulations (thick) and data for a set of relaxed clusters (thin) [7]. Simulations with cooling and star formation feedback are favored.

from the ICM out to the virial radius for $z \lesssim 0.3$ and to R_{500}[1] at higher redshift. X-ray spectroscopy jointly measures the ICM metallicity and temperature, but requires high X-ray fluxes (low z and/or small R). The thermal Sunyaev-Zeldovich effect arises from Compton scattering of CMB photons with the free electrons in the ICM and is proportional to the electron pressure integrated along the line of sight. tSZ imaging is beginning to provide precise pressure profiles out to large radius. Figure 2 displays some recent data, showing how X-ray and tSZ measurements can now map the ICM to a significant fraction of the virial radius rather than being limited to the luminous but complicated core.

The second area consists of observations that quantify non-self-similar phenomena. Gravitational lensing (O/IR imaging) and the galaxy velocity field (O/IR spectroscopy) measure the gravitational well, revealing non-self-similar mass substructure (*e.g.*, mergers). Imaging and spectroscopy from radio to X-ray wavelengths reveal stellar winds and AGN jets and measure AGN and star formation activity and metal enrichment in member galaxies, thereby constraining energy and entropy injection into the ICM. They also catalog the baryons in

[1] R_{500} is the radius at which the average density of the enclosed region is 500 times the critical density of the universe and which typically corresponds to approximately $0.5\,R_{vir}$ for clusters.

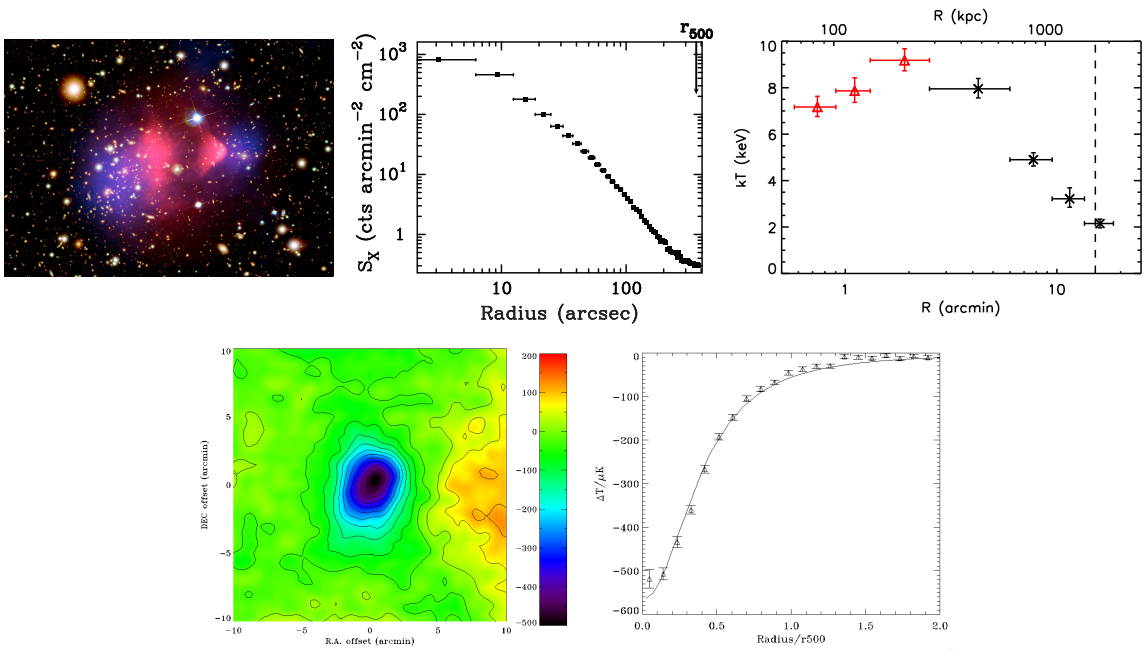

Figure 2: A sample of current X-ray and tSZ data. Top left: Optical, weak lensing (blue), and X-ray (red) image of the Bullet Cluster, $7.5' \times 5.4'$ [1]. Top middle: Chandra X-ray profile of Abell 1835 [8]. Top right: Chandra ($\triangle$'s) and Suzaku ($\times$'s) temperature profiles of PKS0745-191 ($z = 0.10$), vertical line is R_{vir} [9]. Bottom: SPT tSZ image and radial profile of the Bullet Cluster, courtesy of B. Benson/SPT Collaboration. The curve is the best-fit spheroidal beta model.

stars and detect projection effects. Radio synchrotron emission reveals the energy density in magnetic fields and cosmic rays [11, 12, 13] (see white paper by Rudnick *et al.* [14]). Hard X-ray and γ-ray observations will contribute, soon, too.

The third area is simulations to test whether the above phenomena explain observed deviations from self-similar behavior. Simulations (*e.g.*, [3, 15, 7]) have demonstrated the shortcomings of the beta model [10], explained the remarkably regular behavior of the ICM outside cluster cores, shown the existence of and explained ICM temperature gradients, etc. Including radiative cooling and star formation has reduced the discrepancies between simulations and data (Figure 1) [7, 16]. However, differences remain, such as the deficit in the cluster baryon budget (see white paper by Kravtsov *et al.* [17]), the "cooling flow" problem (lack of cool gas in cluster cores), and "overcooling" (too large a stellar mass fraction at large radius in simulations). New simulations will model larger volumes at higher resolution, will include more non-self-similar, "sub-grid" physics, and will enable tests for systematic effects such as He sedimentation or non-equipartition of electrons and protons in cluster outskirts.

New Prospects for Studying the ICM

The question posed here — what is the thermodynamic state of the ICM — is timely because it is now becoming possible to obtain precise X-ray and tSZ imaging out to the virial radius and coming instrumentation will provide higher angular resolution in tSZ, approaching that of X-ray data. Other white papers address new frontiers in studying the underlying dark matter and in multiwavelength studies of non-self-similar phenomena.

Thermal Sunyaev-Zeldovich Effect

Work into the late 1990s provided unambiguous measurements of the tSZ effect [18, 19, 20, 21, 22, 23]. The first sample of tens of clusters with spatially resolved tSZ signal has been published in the last decade [24, 25, 6]. The key gains in the coming decade will be in sensitivity, sample size, angular resolution, and spatial dynamic range. However, such gains present competing requirements that no single facility can adequately satisfy; a diversity of instrumentation is required to exploit tSZ on scales from arcseconds to half a degree.

Many of the frontiers are being pushed by wide-field bolometric cameras fielded on the South Pole Telescope (SPT) and Atacama Cosmology Telescope (ACT). They are surveying hundreds to thousands of square degrees to a largely redshift-independent mass limit of approximately 2×10^{14} $M_\odot$. The resulting sample of hundreds to thousands of clusters will be nearly complete out to the earliest epoch of cluster formation, providing a unique sample to study the evolution of the ICM. With large fields of view and fast scanning, SPT and ACT have overcome the long-standing technical challenge of simultaneously obtaining high sensitivity, angular resolution good enough to resolve clusters, and access to virial scales.

A complementary group of instruments are following up known clusters. The Sunyaev-Zeldovich Array (SZA) is a close-packed, small-dish interferometer that recovers tSZ flux on scales of $5'$ to $10'$ at an angular resolution of $2'$. It has mapped tens of known clusters [26, 8, 27]. APEX-SZ, LABOCA, AzTEC/ASTE, Bolocam/CSO, and MKIDCam/CSO use imaging detector arrays to map similar numbers of clusters with comparable spatial dynamic range by using scanning techniques that efficiently cover single cluster fields. These instruments also provides access to well-studied equatorial regions not visible to SPT.

New instrumentation will push the resolution frontier. SZA has merged with CARMA and will provide higher angular resolution with comparable spatial dynamic range (Figure 3). MUSTANG/GBT (operational) and AzTEC/LMT (expected 2009) provide comparable resolutions of a few arcseconds. High-resolution tSZ imaging possesses more sensitivity to very hot gas than X-ray imaging and thus is complementary; *e.g.*, SCUBA/Nobeyama imaging of RXJ1347-1145 [28, 29] revealed a previously unsuspected $T > 20$ keV shock. Higher resolution will reveal how ICM fine-scale structure exhibits itself in pressure. Later in the decade, LWCam/CCAT and next-generation instruments on GBT and LMT (TolTEC) will provide high angular resolution over fields-of-view comparable to cluster virial radii. LWCam/CCAT and CIX/LMT will use wide wavelength coverage to separate dusty submm galaxies and cluster tSZ and may be able to use the kinetic SZ effect (Doppler shift due to motion of the CMB scattering medium) to study cluster bulk motions and ICM velocity structure. The major interferometer efforts in the next decade, ALMA and EVLA, will image high-contrast small-scale structure in tSZ with an angular resolution of arcseconds over small fields ($\sim 1'$) in compact configurations, beginning to match Chandra resolution and studying the pressure in clumps, filaments, and shocks.

X-Ray Capabilities

The International X-ray Observatory (IXO) will provide a quantum leap in X-ray capabilities (launch ∼2020; see white paper by Vikhlinin *et al.* [30]). IXO will measure cluster X-ray brightness, temperature, metallicity, and velocity structure to high precision out to the virial radius in a single, moderate-exposure pointing, providing information on plasma turbulence and testing for systematics in temperature measurements based on assumed metallicities.

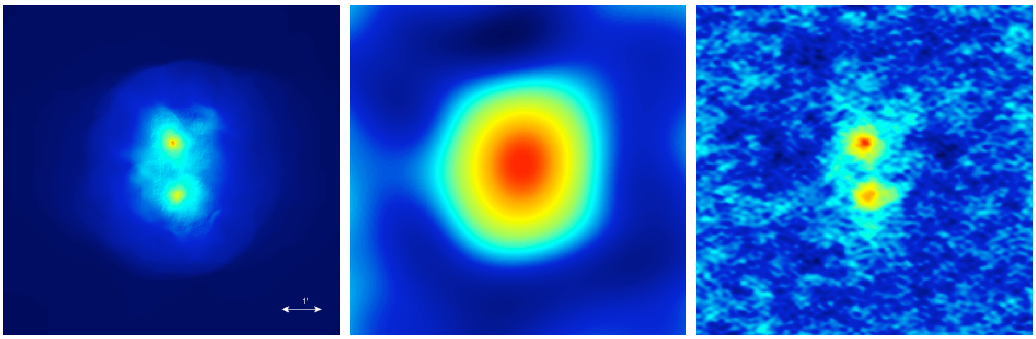

Figure 3: Simulations of low and high-resolution SZ imaging. Left: merging clusters (simulation provided by D. Nagai), $z = 0.25$, $M = 1.7 \times 10^{14}$ $M_\odot$. Middle: SZA 30 GHz. Right: SZA+CARMA 30 GHz. Figure courtesy of E. Leitch.

Prior to IXO, continued use of XMM/Newton, Chandra, and Suzaku and the upcoming intermediate-size missions Spectrum-RG and NeXT/Astro-H will yield useful gains. Suzaku provides a new capability to measure X-ray spectroscopic temperature out to R_{vir} at low z ($z \approx 0.1$ [9]). Spectrum-RG/eROSITA will substantially improve upon the ROSAT All-Sky Survey and will be useful in conjunction with large tSZ surveys, but is comparable to existing missions for sensitivity to emission at large radius, as will be NeXT/Astro-H's wide-field imager. However, NeXT/Astro-H's imaging spectrometer may enable study of ICM velocity structure and spatial metallicity variations at lower X-ray fluxes.

Non-Parametric Cluster Studies

To date, X-ray and tSZ observations have depended on models for interpretation, initially the beta model [18, 19, 20, 22, 23, 24, 25, 6, 26] and, more recently, simulation-derived models [8]. Upcoming work will enable non-parametric study of the ICM via deprojection techniques: assuming a monotonic ellipsoidal ICM structure and using high-resolution X-ray data to remove subclumps and filaments, one can reconstruct from X-ray and tSZ data the density, temperature, orientation, and asphericity [31, 32, 33, 34]. Deprojection has been applied in tSZ work for the first time to recover density and temperature out to R_{500} (Figure 4) [35]. Such analyses can also reveal merging activity and departures from hydrostatic equilibrium. Figure 4 shows the remarkable precision expected for future work of this type.

Feedback from ICM Studies to Galaxy Formation

Comparing and contrasting cluster galaxies with field galaxies will aid in determining the impact of environment on galaxy formation and evolution. Cluster cores are unique environments that result in formation of the most massive galaxies and black holes in the universe, providing extreme test cases for models. Studying the ICM provides information on this environment and measures the impact of galaxies on the ICM, both of which are useful inputs to and tests of galaxy evolution modeling.

Recommendations

A wide variety of facilities are needed for the above studies. Spectrum-RG/eROSITA (launch 2011), SPT (active), and ACT (active) require sufficient support to fully exploit their capabilities. Moreover, they will provide enormous cluster samples that will require followup. NeXT/Astro-H (Phase B, launch 2013) and IXO (in development) are necessary for spec-

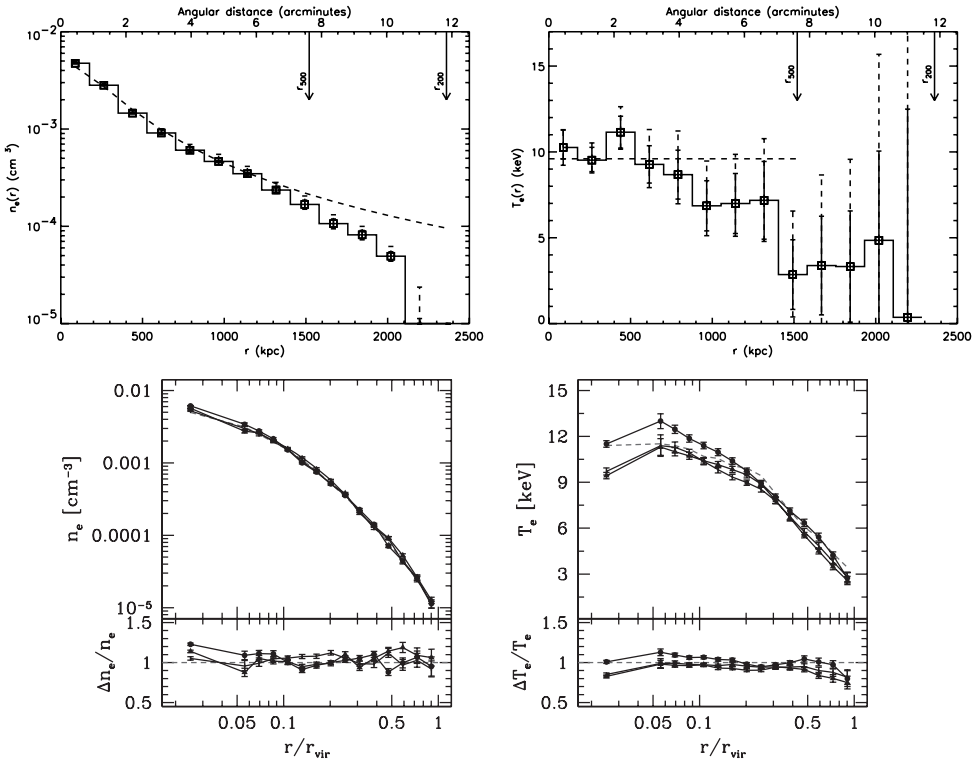

Figure 4: Top: Deprojected density and temperature for A2163 ($z = 0.2$) based on data from XMM/Newton (X-ray), APEX-SZ (tSZ), and LABOCA (tSZ and submm) [35]. The dashed line in the top left figure is a beta model fitted to the central electron density, indicating a discrepancy at large R. The dashed line in the right figure is the best-fit isothermal value. The solid and dashed error bars indicate statistical and systematic (deconvolution) errors, respectively. Bottom: Simulated deprojected density and temperature based on expected LWCam/CCAT sensitivity for a cluster at $z = 0.6$ with simulation-derived error bars (correlated between bins) for three different lines of sight [34]. The dashed line indicates the true radial profile.

troscopy and imaging to large radius. Compact interferometers such as SZA/CARMA (active) and kilopixel bolometer arrays on larger aperture telescopes like CCAT, LMT, and GBT (all in development) will offer the combination of resolution and brightness sensitivity necessary to study tSZ substructure, but support must be provided for technology development, construction, and operations. Support for EVLA compact E-array tSZ observations will also aid in high-resolution work. ALMA requires a 30 GHz receiver system (not in initial construction baseline) to obtain the brightness sensitivity needed to do high resolution followup of the SPT/ACT cluster samples inaccessible to the higher-resolution northern instruments. Given the sophisticated data sets and panchromatic nature of the studies, robust analysis support for existing and future data sets is also required.

References

[1] D. Clowe *et al.*, Astrophys. J. Lett. **648**, L109 (2006).

[2] S. T. Myers *et al.*, *Galaxy Cluster Astrophysics and Cosmology: Questions and Opportunities for the Coming Decade*, Decadal Science White Paper (2009).

[3] P. M. Motl *et al.*, Astroph. J. Lett. **623**, L63 (2005).

[4] A. V. Kravtsov *et al.*, Astroph. J. **650**, 128 (2006).

[5] G. B. Poole *et al.*, Mon. Not. Roy. Astron. Soc. **380**, 437 (2007).
[6] M. Bonamente *et al.*, Astroph. J. **675**, 106 (2008).
[7] D. Nagai *et al.*, Astroph. J. **668**, 1 (2007).
[8] T. Mroczkowski *et al.*, astro-ph/0809.5077.
[9] M. R. George *et al.*, astro-ph/0807.1130 .
[10] A. Cavaliere and R. Fusco-Femiano, Astron. Astroph. **49**, 137 (1976).
[11] E. Nakar *et al.*, Astroph. J. **675**, 126 (2008).
[12] S. Ando and D. Nagai, Mon. Not. Roy. Astron. Soc. **385**, 2243 (2008).
[13] S. W. Skillman *et al.*, Astroph. J. **689**, 1063 (2008).
[14] L. Rudnick *et al.*, *Cluster and Large-Scale Structure: The Synchrotron Keys*, Decadal Science White Paper (2009).
[15] E. J. Hallman *et al.*, Astroph. J. **665**, 911 (2007).
[16] J. O. Burns *et al.*, Astroph. J. **675**, 1125 (2008).
[17] A. Kravtsov *et al.*, *Towards the 2020 vision of the baryon content of galaxy groups and clusters across cosmic time*, Decadal Science White Paper (2009).
[18] W. L. Holzapfel *et al.*, Astroph. J. **480**, 449 (1997).
[19] P. D. Mauskopf *et al.*, Astroph. J. **538**, 505 (2000).
[20] B. S. Mason and S. T. Myers, Astroph. J. **540**, 614 (2000).
[21] E. Komatsu *et al.*, Astroph. J. **516**, L1 (1999).
[22] B. A. Benson *et al.*, Astroph. J. **592**, 674 (2003).
[23] B. A. Benson *et al.*, Astroph. J. **617**, 829 (2004).
[24] S. J. LaRoque *et al.*, Astroph. J. **652**, 917 (2006).
[25] M. Bonamente *et al.*, Astroph. J. **647**, 25 (2006).
[26] S. Muchovej *et al.*, Astroph. J. **663**, 708 (2007).
[27] D. Marrone, private communication.
[28] E. Komatsu *et al.*, Proc. Astron. Soc. Japan. **53**, 57 (2001).
[29] T. Kitayama *et al.*, Proc. Astron. Soc. Japan. **56**, 17 (2004).
[30] A. Vikhlinin *et al.*, Decadal Science White Paper (2009).
[31] K. Yoshikawa and Y. Suto, Astroph. J. **513**, 549 (1999).
[32] J. Lee and Y. Suto, Astroph. J. **601**, 599 (2004).
[33] E. Puchwein and M. Bartelmann, Astron. Astroph. **474**, 745 (2007).
[34] S. Ameglio *et al.*, Mon. Not. Roy. Astron. Soc. **382**, 397 (2007).
[35] M. Nord *et al.*, astro-ph/0902.2131.